J Sol-Gel Sci Technol (2007) 43:21–26
DOI 10.1007/s10971-007-1546-6

ORIGINAL PAPER

Spherical hybrid silica particles modified by methacrylate groups

Eduardo J. Nassar · Evelisy C. de O. Nassor · Lilian R. Ávila · Paula F. S. Pereira · Alexandre Cestari · Luiz M. Luz · Katia J. Ciuffi · Paulo S. Calefi

Received: 25 April 2006 / Accepted: 30 January 2007 / Published online: 13 April 2007

Abstract Organic–inorganic hybrid materials have been used as fillers to reinforce dental resin composites, which require strengthening to improve their performance in large stress-bearing applications such as crowns and multiple-unit restorations. Homogeneous organic–inorganic hybrid materials with high performance were prepared by mixing 3-methacryloxypropyltrimethoxysilane (MPTS) and tetraethylorthosilicate (TEOS) synthesized by the sol–gel route. The matrix was prepared by hydrolyzing and condensing the TEOS and MPTS, using basic catalysis and excess water. The resulting xerogel was treated at 50, 100, 150, and 200 °C for 4 h, and the structure was analyzed by thermogravimetry (TG/DTA), photoluminescence (PL), nuclear magnetic resonance (NMR ^{29}Si and ^{13}C), transmission electron microscopy (TEM), infrared spectroscopy (IR), and Raman spectroscopy. The PL spectra displayed the Eu^{3+} lines characteristic of $^5D_0 \rightarrow {}^7F_{J\ (J = 0,\ 1,\ 2,\ 3,\ 4)}$ ions, and the blue emission was ascribed to the silica matrix. TG, MNR and infrared spectroscopy analyses indicated the hybrid silica was stable, with the organic part present up to 150 °C. Increasing the temperature of the heat treatment was found to increase the degree of hydrolysis. The size and morphology of the silica particles were identified by TEM.

Keywords Europium III · Sol–gel · Hybrids · Dental resin composites

E. J. Nassar (✉) · E. C. de O. Nassor · L. R. Ávila · P. F. S. Pereira · A. Cestari · L. M. Luz · K. J. Ciuffi · P. S. Calefi
University of Franca, Av. Dr. Armando Salles Oliveira, 201, 14404-600 Franca, SP, Brazil
e-mail: ejnassar@unifran.br

1 Introduction

Photo-activated dental resin composites, which first appeared in the early 1970s, have been highly successful thanks to their natural color and easy, unrestricted handling time. Based on organic polymers and inorganic materials (fillers), the earliest formulations of these composites presented low resistance due to the shape and size of the filler particles. Whereas organic polymers are flexible and lightweight, with good impact resistance and processability, inorganic materials have high mechanical strength and good chemical resistance, thermal stability, and optical properties [1]. Hybrid materials obtained by the sol–gel route combine the advantages of both organic and inorganic properties. Several kinds of precursors of organofunctional alkoxysilanes have been studied in the preparation of silicon nanoparticles. These precursors present bifunctional properties in resin composites with dual characteristics, such as aminoalkoxysilane [2, 3], chloroalkoxysilane [4], methacrylatealkoxysilane [5], glycidylalkoxysilane [3], polydimethylsiloxanes [6], and others [7–10].

Inorganic fillers have little affinity for organic polymers due to the hydrophilic nature of these polymers. However, these materials can interact when crosslinking agents are used at the surface of the inorganic layer. Alkoxysilane can be used to confer this characteristic, serving as an interface between organic and inorganic phases by forming hydrogen bonds, electrostatic interactions, and covalent bonds [11]. This is an important point because, due to their physical properties, organofunctional silanes such as 3-methacryiloxypropyltrimethoxysilane (MPTS) are used on an industrial scale as adhesion promoters, surface-modifying agents, crosslinking agents, and as mechanical reinforcements for ceramic surfaces [3, 12].

The sol–gel process is based on the hydrolysis and condensation of metal or silicon alkoxides and is used to obtain a variety of high purity inorganic oxides that are simple to prepare [13, 14]. This process can be employed to obtain and prepare functionalized silica with controlled particle size and shape [2–4, 15, 16].

In this work, high performance homogeneous organic–inorganic hybrid materials were prepared by mixing 3-methacryloxypropyltrimethoxysilane (MPTS) and tetraethylorthosilicate (TEOS) synthesized by the sol–gel route. The matrix was prepared by the hydrolysis and condensation of TEOS and MPTS, using basic catalysis and excess water. The resulting xerogel structure was analyzed by thermogravimetry (TG/DTA), photoluminescence (PL), magnetic nuclear resonance (NMR ^{29}Si and ^{13}C), transmission electron microscopy (TEM), and infrared spectroscopy.

2 Experimental

The material was synthesized by the sol–gel route. The sample was prepared in a molar ratio of 1:1 tetraethylorthosilicate (TEOS): 3-methacryloxypropyltrimethoxysilane (MPTS). 1.00 mL of TEOS and 1.06 mL of MPTS in 0.5 mL of dry ethanol was added to the solution under magnetic stirring at room temperature, and a saturated ethanol ammonium solution was used as catalyst. After 40 min of stirring, the solvent was evaporated at room temperature for 1 week. The resulting material was heat-treated at 50, 100, 150, and 200 °C for 4 h.

Thermal Analysis (TG/DTA/DSC) was carried out in a thermal analyzer (TA Instruments, SDT Q600, Simultaneous DTA-TG) under a nitrogen atmosphere and at a heating rate of 20 °C min^{-1}, from 25 °C to 1,500 °C.

The luminescence data was obtained with a Spex Fluorolog II spectrofluorometer at room temperature. The emission was collected at 22.5° (front face) from the excitation beam.

^{29}Si and ^{13}C were subjected to NMR (59.5 MHz) with an INOVA 300 Varian spectrophotometer, using silicon nitride as reference.

The morphology of the system was investigated by transmission electron microscopy (TEM) of a drop of suspension deposited on a copper grid. The TEM analysis was performed with a 200 kV Philips CM 200 microscope.

Infrared spectra from KBr pellets were obtained with a Nicolet Protege 460 spectrophotometer.

3 Results and discussion

Figure 1 shows the thermogravimetric curve (TG) and derivate (DTG) of the samples containing a 1:1 molar ratio of TEOS and MPTS, dried at room temperature (~25 °C).

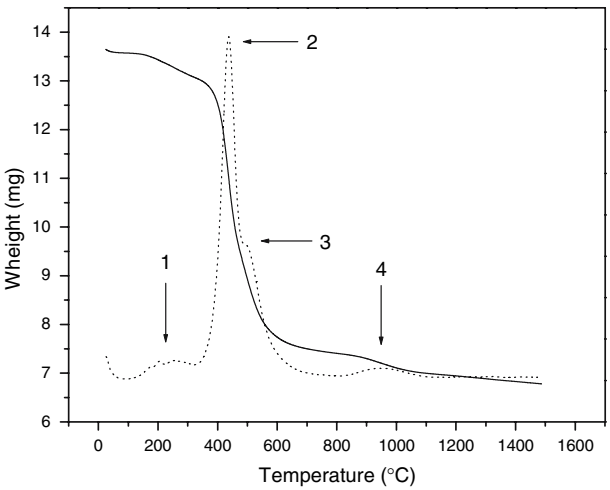

Fig. 1 TG and DTG curves of the sample dried at room temperature

The curve presents four distinct weight losses. The first, which occurs between 100 °C and 300 °C, can be ascribed to water and solvent molecules while the second and third, which take place between 300 °C and 700 °C, may be due to the methacrylate group. The fourth appears between 800 °C and 1,000 °C, and can be ascribed to structural changes and loss of residual organic molecules.

The silica was prepared in a molar ratio of 1:1 TEOS:MPTS. The theoretical calculations and experimental data showed a complete convergence, indicating that organic molecules comprised 49% of the hybrid organic–inorganic mass. Our TG analysis indicated that the maximum temperature of thermal stability was 300 °C, and the samples were treated at temperatures of 50, 100, 150, and 200 °C. Table 1 shows the percentage of mass loss as a function of temperature.

The TG curve of the samples treated at 25, 50, and 100 °C showed a similar behavior, which was ascribed to the methacrylate groups. Treating the samples at 150 °C and 200 °C caused a change in behavior, possibly due to the onset of the decomposition of the organic group. Xiong et al. [1] reported that the maximum decomposition temperature of the organic group in MPTS was 401 °C; however, in our study, the maximum temperature for this decomposition was 439 °C, without titanium particles.

Table 1 Percentage of mass loss as a function of treatment temperature

Sample (°C)	Organic molecules (%)
25	49.8
50	49.8
100	49.3
150	52.4
200	48.8

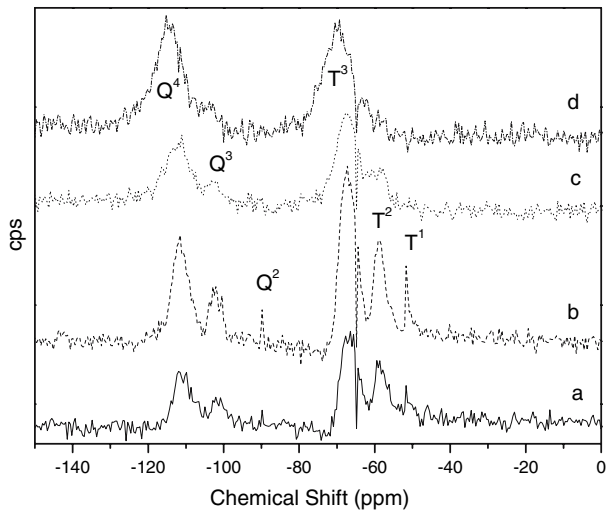

Fig. 2 ^{29}Si NMR spectrum of the sample dried at: (a) 25 °C, (b) 100 °C, (c) 150 °C, and (d) 200 °C

NMR of ^{29}Si allows for the analysis of the chemical environment of silicon atoms in samples. The Si-atoms, which are bound to four oxygen atoms, can be represented by a tetrahedron whose corners link to other tetrahedra. The Q^n notation serves to describe the substitution pattern around a specific silicon atom, with Q representing a silicon atom surrounded by four oxygen atoms and ^{n} indicating the connectivity. In this study, ^{29}Si NMR was used to analyze hybrid materials produced by condensation of alkyltrialkoxysilanes. The notation (T^n), the signal corresponding to the respective T^n sites, shifts approximately 40 ppm down field for every alkoxy substituent that is replaced by an alkyl group [17]. Figure 2 presents the NMR spectrum of the samples dried at room temperature (25 °C), 100, 150, and 200 °C.

The material presented peaks corresponding to the Q^4, Q^3, and Q^2 sites at –110, –102, and –90 ppm, respectively and T^3, T^2, and T^1 sites at –67, –58, and –51 ppm, respectively. Table 2 presents the sample's silicon sites and chemical shifts.

We found that the degree of hydrolysis was temperature-dependent, since the sample treated at 200 °C presented only T^3 and Q^4, indicating total hydrolysis of the alkoxide groups. The T^3 site indicated the presence of the organic group in the hybrid materials.

Table 2 Silicon sites in the samples containing TEOS and MPTS treated at different temperatures

Samples (°C)	T^1	T^2	T^3	Q^1	Q^2	Q^3	Q^4
25	–51	–58	–66	–	–90	–101	–111
100	–51	–58	–67	–	–90	–102	–111
150	–	–58	–68	–	–	103	–110
200	–	–	–70	–	–	–	–115

The integrity of the organic group can be assessed by NMR ^{13}C prior to heat treatment. The NMR ^{13}C spectra presented several chemical shifts due to different carbon species. The chemical shifts at 10 ppm were ascribed to carbon bound to silicon atoms, whose peak appeared in all the spectra. New peaks at 45 ppm and 54 ppm appeared in the samples treated at 150 °C and 200 °C, indicating the formation of new species originating during decomposition of the organic matter. The samples treated at 25 °C and 100 °C showed chemical shifts at 126 ppm and 137 ppm, which are peaks are characteristic of alkenes [18, 19]. These peaks were absent from the samples treated at 150 °C and 200 °C due to breakdown of the double bond.

TEM can give structural information about materials, such as particle shape and size. Figure 3a and b shows TEM images of the samples treated at 25 °C and 200 °C.

These TEM images revealed the formation of spherical particles with an average size of 3 μm. The material between the silica particles was ascribed to the organic groups, which appeared in both images but increased at 25 °C due to partially hydrolyzed precursors. Energy-dispersive X-ray spectroscopy (EDX) analyses confirmed the presence of carbon atoms in these materials.

The sample treated at 200 °C presented particles not totally spherical and 10% smaller than those of the samples dried at room temperature, probably due to loss of solvent and water molecules.

The IR spectra of the samples treated at several temperatures are shown in Fig. 4.

In the literature, the bands in the infrared (IR) region that are attributed to chemically bound water appear at 3,740 cm^{-1} of the spectrum, while stretching vibrations of the Si–OH group appear at 3,650 cm^{-1} for neighboring or interacting silanols (wide band), and adsorbed water appears at 3,400 cm^{-1} [20, 21]. Peaks at 2,980 cm^{-1} and 2,930 cm^{-1} correspond to C–H symmetric stretching vibrations, while peaks at 1,710 cm^{-1} and 1,690 cm^{-1} correspond to the C=O and C=C stretching vibration, respectively. The wide band between 1,070–1,020 cm^{-1} and 1,150–1,110 cm^{-1} corresponds to Si–O–Si and Si–O–C stretching vibrations, respectively. The Si–O vibration band of TEOS appears at 955 cm^{-1} [19, 22].

The spectra in Fig. 4 show peaks at 3,752, 3,440, 2,954, 2,893, 1,727, 1,638, 1,200–990, and 937 cm^{-1}. Among these, the peaks at 3,752 cm^{-1} and 3,440 cm^{-1} correspond to O–H of the water and ethanol (solvent) stretching vibrations. The peaks at 2,954 cm^{-1} and 2,893 cm^{-1} were ascribed to symmetric C–H of the methacrylate group, present in all the samples. The peaks at 1,727 cm^{-1} and 1,638 cm^{-1} correspond to C=O and C=C stretching vibrations, respectively. The peak at 937 cm^{-1} appeared only in

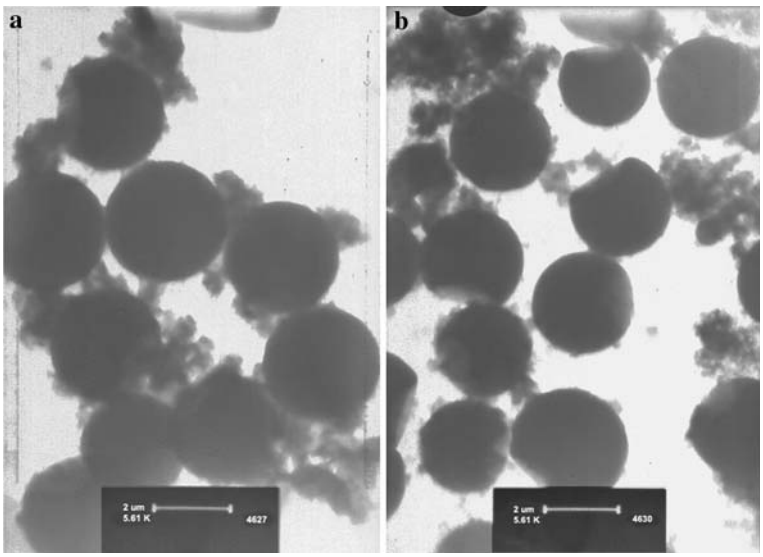

Fig. 3 TEM images of the samples treated at 25 °C (**a**) and 200 °C (**b**)

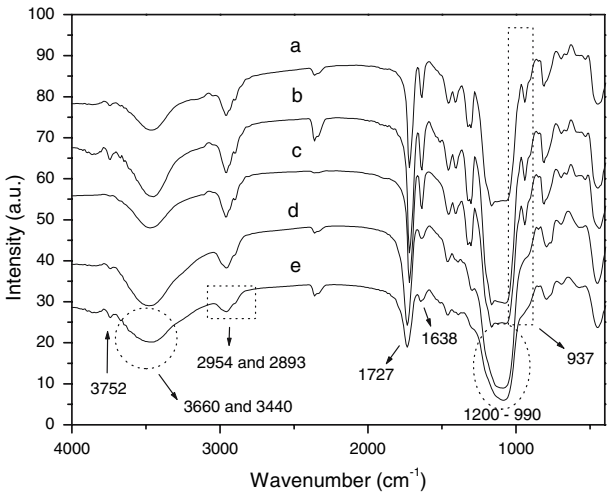

Fig. 4 IR spectra of the samples treated at: (a) room temperature (25 °C), (b) 50 °C, (c) 100 °C, (d) 150 °C, and (e) 200 °C

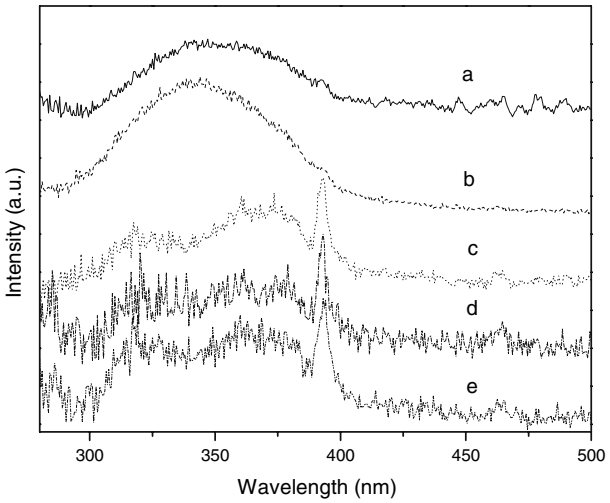

Fig. 5 Excitation spectra of the Eu III ion doped in silica matrix treated at different temperatures; (a) 25 °C, (b) 50 °C, (c) 100 °C, (d) 150 °C, and (e) 200 °C

samples treated at 25, 50, and 100 °C, disappearing at higher temperatures due to the increased degree of hydrolysis as a function of temperature, as evidenced by the NMR results.

Figure 5 shows the excitation spectra of the Eu III ion doped in silica matrix and obtained with TEOS and MPTS alkoxides. The maximum emission was found to occur at 612 nm ($^5D_0 \rightarrow {}^7F_2$). The band ascribed from $^7F_0$ (fundamental level) to $^5L_6$ (excitation level) was observed in only three samples treated at 25, 50, and 100 °C. The samples treated at 150 °C and 200 °C showed a wide band at 340 nm.

Figure 6 shows the emission spectra of Eu III ions doped in the matrix, where the excitation wavelength was in the charge transfer band (CTB).

The emission spectra presented transitions arising from $^5D_0$ to ^7F_j (J = 0, 1, 2, 3, and 4) manifolds, and a wide band in the blue region of the electromagnetic spectra when the samples were at maximum excitation. The Eu III emission bands in these spectra are characterized by non-homogenous distributions of the ion in the silica matrix [23–25]. The band corresponding to $^5D_0 \rightarrow {}^7F_0$ transitions at 579 nm is due to sites without inversion centers occupied by Eu III ions.

Figures 7 and 8 depict the emission spectra of the samples excited at the $^5L_6$ (393 nm) and $^5D_2$ (420 nm) levels, respectively.

The emission spectra of the samples excited at 393 nm show bands corresponding to the transition of excited states

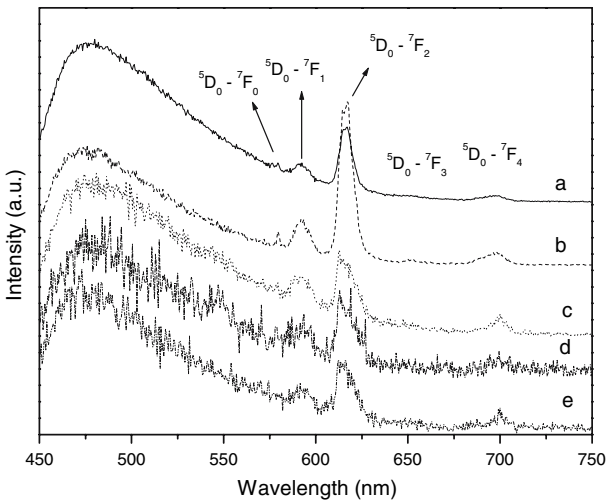

Fig. 6 Emission spectra of the Eu III ion doped in silica matrix treated at different temperatures; (a) 25 °C; $\lambda_{exc.}$ = 317 nm, (b) 50 °C; $\lambda_{exc.}$ = 320 nm, (c) 100 °C; $\lambda_{exc.}$ = 320 nm, (d) 150 °C; $\lambda_{exc.}$ = 344 nm, and (e) 200 °C; $\lambda_{exc.}$ = 347 nm

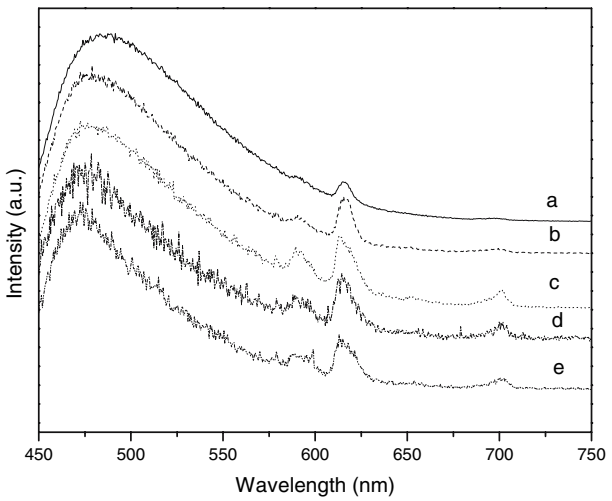

Fig. 7 Emission spectra of the Eu III ion doped in silica matrix treated at different temperatures; (a) 25 °C, (b) 50 °C, (c) 100 °C, (d) 150 °C, (e) 200 °C. $\lambda_{exc.}$ = 393 nm

($^5D_0$) to fundamental states (^7F_J) (J = 0, 1, 2, 3, and 4). When the samples were excited at 420 nm, the Eu III emission disappeared, possibly indicating an energy transfer from Eu III to the matrix, resulting in the matrix emission. The wide band in the blue region of the electromagnetic spectrum was ascribed to inorganic silica [23]. The maximum of the wide band may depend on the excitation wavelength, which is characteristic of matrix emission [26, 27]. Tables 3 and 4 show the emission maxima of the wide band when excited at 393 nm and 420 nm, respectively.

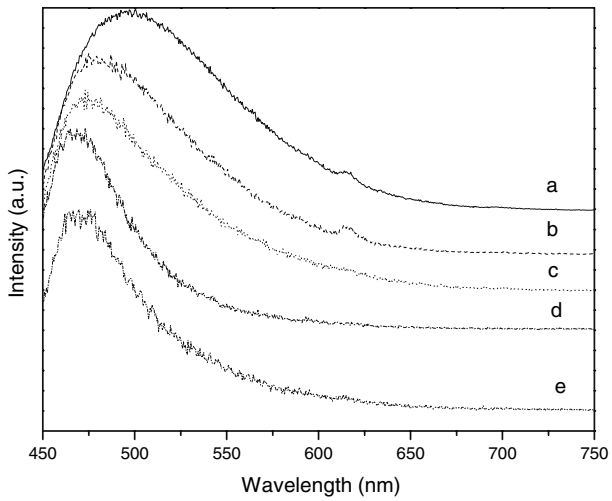

Fig. 8 Emission spectra of the Eu III ion doped in silica matrix treated at different temperatures; (a) 25 °C, (b) 50 °C, (c) 100 °C, (d) 150 °C, (e) 200 °C. $\lambda_{exc.}$ = 420 nm

Table 3 Emission maxima of the wide band when excited at 393 nm

Sample	25 °C	50 °C	100 °C	150 °C	200 °C
λ (nm)	472	476	478	480	486

Table 4 Emission maxima of the wide band when excited at 420 nm

Sample	25 °C	50 °C	100 °C	150 °C	200 °C
Maximum (nm)	469	470	474	480	496

The increase in wavelength is an indication of a major incorporation of the ion into the matrix lattice [27].

4 Conclusions

The thermal analysis in this study revealed the stability of organic molecules bound to the matrix at 150 °C. Modified hybrid organic–inorganic materials have a potential for use in several applications, depending on the precursors used in their preparation. In this case, the stability of the methacrylate group is very important for its application as dental resin. The presence of the –OH group in the silica matrix can lead to incomplete polymerization of the resin. The degree of hydrolysis of the silica matrix obtained by the sol–gel route can be controlled. In this case, we found that the degree of hydrolysis increased with temperature, although the methacrylate group was not affected. Another important aspect is the shape of particles. In this study we obtained almost spherical particles, which favor the formation of dense materials.

The technique used in this investigation indicates that the sol–gel process is an efficient method to obtain different materials based on an inorganic matrix with modified organic molecules.

Acknowledgements The authors acknowledge FAPESP, CNPq and CAPES (Brazilian research funding agencies) for their financial support of this work.

References

1. Xiong M, Zhou S, Wu L, Wang B, Yang L (2004) Polymer 45:8127
2. Nassar EJ, Ciuffi KJ, Ribeiro SJL, Messaddeq Y (2003) Mater Res 6(4):557
3. Beari F, Brand M, Jenkner P, Lehnert R, Metternich HJ, Monkiewicz J, Siesler HW (2001) J Organo Chem 625:208
4. Nassar EJ, Neri CR, Calefi PS, Serra OA (1999) J Non-Cryst Solids 247:124
5. Halvorson RH, Erickson RL, Davidson CL (2003) Dental Mater 19:27
6. Julian B, Beltrán H, Cordoncillo E, Escribano P, Viana B, Sanchez C (2003) J Sol-Gel Sci Techn 26:977
7. Uricanu V, Donescu D, Banu AG, Serban S, Olteanu M, Dudau M (2004) Mater Chem Phys 85:120
8. Yoshinaga I, Yamada N, Katyama S (2003) J Sol-Gel Sci Techn 28:65
9. Wang E, Chow K-F, Kwan V, Chin T, Wong C, Bocarsly A (2003) Analy Chim Acta 295:45
10. Niida H, Takahashio M, Uchino T, Yoko T (2003) J Ceramic Soc Japan 111(3):0171
11. Philipse AP, Vrij A (1989) J Coll Inter Sci 128:121
12. Mür E, Marquardt J, Klee JE, Frey H, Mülhaupt R (2001) Macromolecues 34:5778
13. Rocha LA, Ciuffi KJ, Sacco HC, Nassar EJ (2004) Mater Chem Phys 85:245
14. Lobnik A, Majcen N, Niederreiter K, Uray G (2001) Sensors Actuat B 74:200
15. Stöber W, Fink A, Bon E (1968) J Coll Inter Sci 26:62
16. Papacidero AT, Rocha LA, Caetano BL, Molina EF, Sacco HC, Nassar EJ, Martinelli Y, Mello C, Nakagaki S, Ciuffi KJ (2006) Coll Surfaces 275:27
17. Wright JD, Sommerdijk NAJM (2003) Sol–gel materials chemistry and applications. Taylor & Francis
18. Silverstein RM, Webster FX (2000) Em: ''Identificação Espectroscópica de Compostos Orgânicos'', 6ª. Edição, Editora LTC
19. Vinod MP, Bahenemann D, Rajamohanan PR, Vijayamohanan K (2003) J Phys Chem B 107:11583
20. Mitchell SA (1966) Chem Indus 4:924
21. Low MJD, Ramasubramanian N (1967) J Phys Chem 71(3):730
22. King L, Sullivan AC (1999) Coord Chem Rev 189:19
23. Hazenkamp MF, Van der Veen AMH, Feiken W, Blasse G (1992) J Chem Soc Faraday Trans 88(1):141
24. Rice DK, Deshaser LG (1969) Phys Rev B 186:387
25. Reisfeld R (1984) J Eletrochem Soc 131:1360
26. Carlos LD, Ferreira RAS, Bermudez VDZ, Ribeiro SJL (2001) Adv Funct Mater 11(2):111
27. Carlos LD, Bemudez VDZ, Ferreira RAS (1999) J Non-Cryst Solids 247:203